Eapen, A. V., Fernández-Fernández, D., Georgiou, J., Bortolotto, Z., Lightman, S., Jane, D. E., Volianskis, A., & Collingridge, G. L. (2021). Multiple roles of GluN2D-containing NMDA receptors in short-term potentiation and long-term potentiation in mouse hippocampal slices. *Neuropharmacology*, *201*, [108833]. https://doi.org/10.1016/j.neuropharm.2021.108833

Neuropharmacology 201 (2021) 108833

Contents lists available at ScienceDirect

Neuropharmacology

journal homepage: www.elsevier.com/locate/neuropharm

Multiple roles of GluN2D-containing NMDA receptors in short-term potentiation and long-term potentiation in mouse hippocampal slices

Alen V. Eapen [a,b,1,*], Diego Fernández-Fernández [a,1,2], John Georgiou [b], Zuner A. Bortolotto [a], Stafford Lightman [c], David E. Jane [a], Arturas Volianskis [a,c,d], Graham L. Collingridge [a,b,e,f]

[a] Centre for Synaptic Plasticity, School of Physiology, Pharmacology and Neuroscience, University of Bristol, Bristol, UK
[b] Lunenfeld-Tanenbaum Research Institute, Mount Sinai Hospital, Sinai Health System, Toronto, ON, Canada
[c] Bristol Medical School, University of Bristol, Bristol, UK
[d] Centre for Neuroscience, Surgery and Trauma, Blizard Institute, Barts and The London School of Medicine and Dentistry, Queen Mary University of London, UK
[e] Department of Physiology, University of Toronto, Toronto, ON, Canada
[f] TANZ Centre for Research in Neurodegenerative Diseases, University of Toronto, Toronto, ON, Canada

ARTICLE INFO

Keywords:
LTP
Long-term potentiation
Hippocampus
STP
Short-term potentiation
GluN2D knockout mice

ABSTRACT

The GluN2 subunits of N-methyl-D-aspartate receptors (NMDARs) are key drivers of synaptic plasticity in the brain, where the particular GluN2 composition endows the NMDAR complex with distinct pharmacological and physiological properties. Compared to GluN2A and GluN2B subunits, far less is known about the role of the GluN2D subunit in synaptic plasticity. In this study, we have used a GluN2C/2D selective competitive antagonist, UBP145, in combination with a GluN2D global knockout (GluN2D KO) mouse line to study the contribution of GluN2D-containing NMDARs to short-term potentiation (STP) and long-term potentiation (LTP) in the CA1 region of mouse hippocampal slices. We made several distinct observations: First, GluN2D KO mice have higher levels of LTP compared to wild-type (WT) mice, an effect that was occluded by blockade of GABA receptor-mediated inhibition or by using a strong LTP induction protocol. Second, UBP145 partially inhibited LTP in WT but not GluN2D KO mice. Third, UBP145 inhibited a component of STP, termed STP2, in WT but not GluN2D KO mice. Taken together, these findings suggest an involvement for GluN2D-containing NMDARs in both STP and LTP in mouse hippocampus.

1. Introduction

Pharmacological studies using the specific N-methyl-D-aspartate receptor (NMDAR) antagonist D-AP5 (Davies et al., 1981) demonstrated that this subtype of glutamate receptor is important for the induction of long-term potentiation (LTP) at the Schaffer collateral-commissural to CA1 pyramidal cell (SC-CA1) synapses in the hippocampus (Collingridge et al., 1983). Subsequent cloning of the NMDAR identified multiple subunits that can co-assemble in various configurations (Kutsuwada et al., 1992; Meguro et al., 1992; Monyer et al., 1992; Karp et al., 1993). Most NMDARs are composed of two GluN1 subunits and two GluN2 subunits, of which four subtypes exist – GluN2A-D (Collingridge et al., 2009). The subunit composition of the NMDAR imparts distinct functional properties to the receptor, such as its channel kinetics and sensitivity to Mg^{2+} (Monyer et al., 1994; Vicini et al., 1998). Whereas the GluN2A and GluN2B subunits have been extensively studied in LTP (e.g., Sakimura et al., 1995; Liu et al., 2004; Bartlett et al., 2007; Volianskis et al., 2013a) far less is known regarding the roles of the GluN2C and GluN2D subunits in synaptic plasticity.

The development of pharmacological tools has, however, enabled several functions of GluN2D-containing NMDARs in synaptic plasticity to be identified. Notably the development of competitive antagonists by David Jane and his colleagues, in the Bristol laboratory founded by Jeff Watkins, has led to several important insights. An early Bristol compound, (2*R**,3*S**)-1-(phenanthrenyl-2-carbonyl)piperazine-2,3-dicarboxylic acid (PPDA), has 3–10 fold higher selectivity for GluN2C/D vs GluN2A/B (Hrabetova et al., 2000). Its effects on LTP were compared with those of D-3-(2-carboxypiperazine-4-yl)-1-propenyl-1-phosphonic

* Corresponding author. Lunenfeld-Tanenbaum Research Institute, Mount Sinai Hospital, Toronto, Canada.
E-mail address: aeapen@lunenfeld.ca (A.V. Eapen).
[1] Equal contribution.
[2] Present address: Department of Biomedicine, University of Basel, Basel, Switzerland.

https://doi.org/10.1016/j.neuropharm.2021.108833
Received 5 August 2021; Received in revised form 28 September 2021; Accepted 7 October 2021
Available online 9 October 2021

acid (CPP; Davies et al., 1986), which has much higher selectivity for GluN2A/B vs GluN2C/D. On this basis, it was concluded that different NMDAR subtypes mediate the induction of LTP and LTD at CA1 synapses (Hrabetova et al., 2000). PPDA was also used to identify a slow post-synaptic current induced by repetitive stimulation, suggesting that GluN2D-containing NMDARs may contribute to extrasynaptic currents in CA1 neurons (Lozovaya et al., 2004). Next a series of PPDA analogues, including (2*R**,3*S**)-1-(phenanthrene-3-carbonyl)piperazine-2,3-dicarboxylic acid (UBP141) and (2*R**,3*S**)-1-(9-bromophenanthrene-3-carbonyl)piperazine-2,3-dicarboxylic acid (UBP145), were synthesized in the former Watkins' laboratory and found to have greater selectivity as GluN2C/D vs GluN2A/B antagonists (Costa et al., 2009). The use of UBP141 provided additional support for extrasynaptic GluN2D-containing NMDARs activated by repetitive stimulation (Costa et al., 2009).

We have also used UBP145 to investigate the role of GluN2C/D-containing NMDARs in synaptic plasticity at SC-CA1 synapses (Volianskis et al., 2013a; France et al., 2017). We made the following observations: (i) STP can be divided into two kinetically and pharmacologically distinct components, a fast component that is relatively insensitive ($IC_{50} \approx 30$ μM) and a slow component that is highly sensitive ($IC_{50} \approx 2$ μM) to UBP145. We named these two components STP1 and STP2, respectively. (ii) LTP is relatively insensitive to UBP145 ($IC_{50} \approx 30$ μM). (iii) the NMDAR-EPSC has a low sensitivity to UBP145 ($IC_{50} \approx 13$ μM). (iv) The fast and slow exponential components of the NMDAR-EPSC decay are affected similarly by UBP145. (v) In HEK cells, challenged with 15 μM NMDA, receptors containing the GluN2D subunit ($IC_{50} \approx 1$ μM) are >10-fold more sensitive than either GluN2A ($IC_{50} \approx 16$ μM) or GluN2B ($IC_{50} \approx 13$ μM) subunits to UBP145. Based on these observations we concluded that STP2 involves NMDARs containing the GluN2D subunit. We assumed that the relatively low sensitivity of the synaptic current, STP1 and LTP to UBP145 was because of its effects on GluN2A- and/or GluN2B-containing NMDARs at these concentrations. However, we could not exclude the possibility that these actions were also due to an effect on GluN2D-containing NMDARs, perhaps involving the postsynaptic current identified previously (Lozovaya et al., 2004).

Other issues with UBP145 is that it is also active at GluK1-containing kainate receptors ($K_B \approx 13$ μM; Irvine et al., 2012) and displays very little selectivity between GluN2D (1 μM) and GluN2C (3 μM) subunits. To circumvent the issues surrounding the selectivity of UBP145 and to obtain independent evidence for the roles of GluN2D-containing NMDARs in synaptic plasticity we have now combined the use of UBP145 with a global GluN2D KO mouse line, developed by Mishina and colleagues (Ikeda et al., 1995). Our findings reveal multiple roles for GluN2D-containing NMDARs in synaptic plasticity that are distinct from the roles of the GluN2A and GluN2B subunits.

2. Material and methods

2.1. Animals and slice preparation

The global GluN2D KO mice were obtained from Professor Masayoshi Mishina (University of Kyoto) and maintained at a breeding facility in the UK (Charles River). All experiments were performed according to UK Scientific Procedures Act, 1986 and European Union guidelines for animal care. Adult (3–6 months old) wild-type (WT) and GluN2D KO of the C57BL/6 strain were used for field extracellular recordings and 1–2 month old mice were used for voltage-clamp recordings. Mice were anaesthetised with isofluorane and after decapitation, the brain was removed and cooled (0–4 °C) in artificial cerebrospinal fluid (ACSF), which contained (in mM): 124 NaCl, 3.5 KCl, 1.25 NaH_2PO_4, 26 $NaHCO_3$, 2 $CaCl_2$, 2 $MgSO_4$ and 10 glucose, saturated with 95% O_2 and 5% CO_2. Transverse slices (400 μm) of the dorsal hippocampus were cut and incubated at room temperature (~20 °C) for at least 2 h before the start of experiments. During experiments, slices were perfused with ACSF and maintained submerged at 33 °C.

2.2. Chemicals

D-AP5, picrotoxin, (−)-bicuculline methochloride, and CGP 55845 hydrochloride were purchased from Hello Bio Ltd (Bristol, UK). L-689,560 was purchased from Tocris Bioscience (Bristol, UK). UBP145 was synthesized in-house as described previously (Morley et al., 2005; Wang et al., 2020) . The AMPA receptor/kainate receptor antagonist, 2, 3-dihydroxy-6-nitro-7-sulfamoylbenzo(*f*)quinoxaline (NBQX), was purchased from HelloBio (Bristol, UK). All antagonists were prepared as stock solutions, stored as frozen and added to the perfusate. All other chemicals and salts were purchased from Sigma (Dorset, UK) or Fisher Scientific (Loughborough, UK).

2.3. Electrophysiological recordings

Only one slice per animal was used for any given experiment; therefore, all n values apply to both the number of slices and mice. Field-excitatory postsynaptic potentials (fEPSPs) were recorded from the CA1 area of the *stratum radiatum* of the hippocampus after stimulation of the Schaffer collaterals (SCs) using a bipolar concentric platinum core electrode with a tip diameter of 12.5 μm (FHC, Inc, USA). Borosilicate recording electrodes were filled with ACSF and had resistance in the 1.5–2 MΩ range. Stimulus pulses (duration of 0.1 ms) were generated using a stimulus isolating unit (DS2A Mk2; Digitimer Ltd, Hertfordshire, UK). Responses were evoked by stimulating once every 15 s and are presented as averages of four consecutive responses. Baseline stimulation intensity was set to three times the threshold for evoking fEPSPs. LTP was induced, at the same stimulus intensity with one of two protocols both of 2 s duration and consisting of bursts of four stimuli at 100 Hz; the bursts were repeated either every 200 ms (10B = 10-bursts, 40 stimuli in total) or 67 ms (30B = 30-bursts, 120 stimuli in total). After LTP induction, stimulation was paused for 3 min and resumed at the pre-LTP induction frequency (1 per 15 s) to test the potentiation at synapses. Recorded signals were amplified and filtered at 5 kHz (AxoPatch 1D; Axon Instruments, USA), digitized at 40 kHz (National Instruments, USA) and acquired using WinLTP software (Anderson and Collingridge, 2007).

Whole-cell voltage clamp recordings were made from cell bodies of pyramidal cells or stratum radiatum interneurons using differential interference contrast optics and comparing membrane passive properties (Rempe et al., 1997). Patch pipettes were filled with internal solution containing (in mM): 130 $CsMeSO_3$, 8 NaCl, 4 Mg-ATP, 0.3 Na-GTP, 0.5 EGTA, 10 Hepes, 5 QX-314, 10 BAPTA, which had an osmolarity of 280 mOsm and pH of 7.2. Excitatory postsynaptic currents (EPSCs) were evoked every 30 s by extracellular stimulation of SCs in the *stratum radiatum*. NMDAR-mediated EPSCs were isolated by bath application of 3 μM NBQX and 50 μM picrotoxin and voltage clamping the cells at −40 mV. Recordings were made with an Axon 700B amplifier (Axon Instruments) and digitized at a sampling rate of 20 kHz. Only experiments that had <20% change in series resistance (Rs) were included in analysis.

2.4. Data analysis

The fibre volley (FV) was measured as the peak amplitude of the first deflection in the response waveform after the stimulus artifact, and fEPSPs were measured using the slope of the initial rising phase (0.5 ms duration) following the FV. Baseline transmission was assessed using input-output (IO) experiments, in which a series of stimuli at increasing intensity were delivered to the SC axons. The relationship between FV and stimulus intensity, and between fEPSP and FV were assessed by linear regression. Paired-pulse facilitation (PPF) was determined by evoking two fEPSPs with an inter-pulse interval of 50 ms. LTP was calculated as the average potentiation of the last 5 min of recording. The decay of STP was calculated by fitting a bi-exponential function to the averaged data for each pooled data set according to the formula:

$$P = LTP + \left(A_{STP1} \times e^{-t/\tau_1}\right) + \left(A_{STP2} \times e^{-t/\tau_2}\right) \quad (1)$$

P is the total potentiation at time t, LTP is defined above, A_{STP1} and A_{STP2} are the magnitude of the fast and slow phases of STP at t = 0 (4 min post induction), respectively, t is the time since start of decay, τ_1 and τ_2 are time constants of decay of STP1 and STP2, respectively. The contribution of STP1 and STP2 was calculated by integrating the best fit of each exponential component from eq. (1) for individual experiments. Individual STP1 and STP2 values are expressed as normalised values, as indicated in the figures.

Analysis of fEPSPs and EPSCs were performed offline using Platin (Morten Jensen, University of Aarhus, Denmark) and WinLTP (Anderson and Collingridge, 2007). LTP and STP calculations using exponential non-linear regression fitting, statistical comparisons, and plotting were performed using GraphPad Prism 7 (GraphPad Software, Inc., La Jolla, CA, USA). LTP, STP and EPSC amplitude values were compared using Student's t-test and analysis of variance (ANOVA) followed by Bonferroni's multiple comparison test as appropriate. Decay time constant (τ) values of group data were compared using F tests. Statistical significance was set at $P < 0.05$, the level of significance is indicated in the figures (*P < 0.05, **P < 0.01, ***P < 0.001, ****P < 0.0001) and absolute P values are presented in the figure legends.

3. Results

3.1. Baseline synaptic transmission and PPF are similar in WTs and GluN2D KOs

The GluN2D subunit is highly expressed during development (Monyer et al., 1994; Ikeda et al., 1995). We therefore determined whether its constitutive absence has any effect on AMPAR-mediated synaptic transmission. We varied the stimulus intensity and measured the peak FV amplitude and initial slope of the fEPSP (Fig. 1). There was no difference in either the relationship of FV amplitude to stimulus intensity (Fig. 1A, D) or fEPSP slope to FV amplitude (Fig. 1B, D). Furthermore, PPF was also similar (Fig. 1C, E). Therefore, there were no obvious differences between genotypes in basal synaptic properties and short-term presynaptic plasticity, as assessed by PPF.

3.2. STP1 and LTP are enhanced in KOs

In WTs, a single 10-bursts train of theta-burst stimulation (TBS), that comprised 40 stimuli in total, resulted in LTP of 38.6 ± 4.1%, calculated as the level of potentiation averaged over the last 5 min of each experiment. In KOs, this TBS protocol induced a significantly greater LTP of 54.3 ± 5.5% (Fig. 2A). STP has been shown to be comprised of two pharmacologically and kinetically distinct components termed STP1 and STP2 (Volianskis et al., 2013a). The time-constants of decay for the average data of STP1 and STP2 were not significantly different between WTs (3.0 and 24.0 min) and KOs (4.7 min and 25.8 min). To estimate the magnitude of STP1 and STP2, we fitted the average decay to each individual experiment, subtracted LTP and calculated the area under the curve of each decay component. STP1 was significantly greater in KOs compared to WTs (112.4 ± 19.4% increase), whereas STP2 was not significantly different between genotypes (38.7 ± 15.7% increase; Fig. 2B).

GluN2D-containing NMDARs contribute to the excitatory drive of GABA interneurons in the CA1 region (Perszyk et al., 2016; Swanger et al., 2018; Yi et al., 2019). We therefore investigated whether the enhanced synaptic potentiation in KOs may be due to changes in GABA-mediated synaptic transmission (Fig. 2C). In the presence of $GABA_A$ and $GABA_B$ receptor antagonists, LTP was similar in KOs (67.4 ± 10.7%) and WTs (79.4 ± 8.1%). The time constants of decay of STP1 and STP2 were similar in KOs (τ_1 = 2.1 min, τ_2 = 25.1 min) and WTs (τ_1 = 1.7 min, τ_2 = 19.2 min). However, STP1 was significantly greater in KOs (91.6 ± 32.2% increase) whereas STP2 was significantly less in KOs

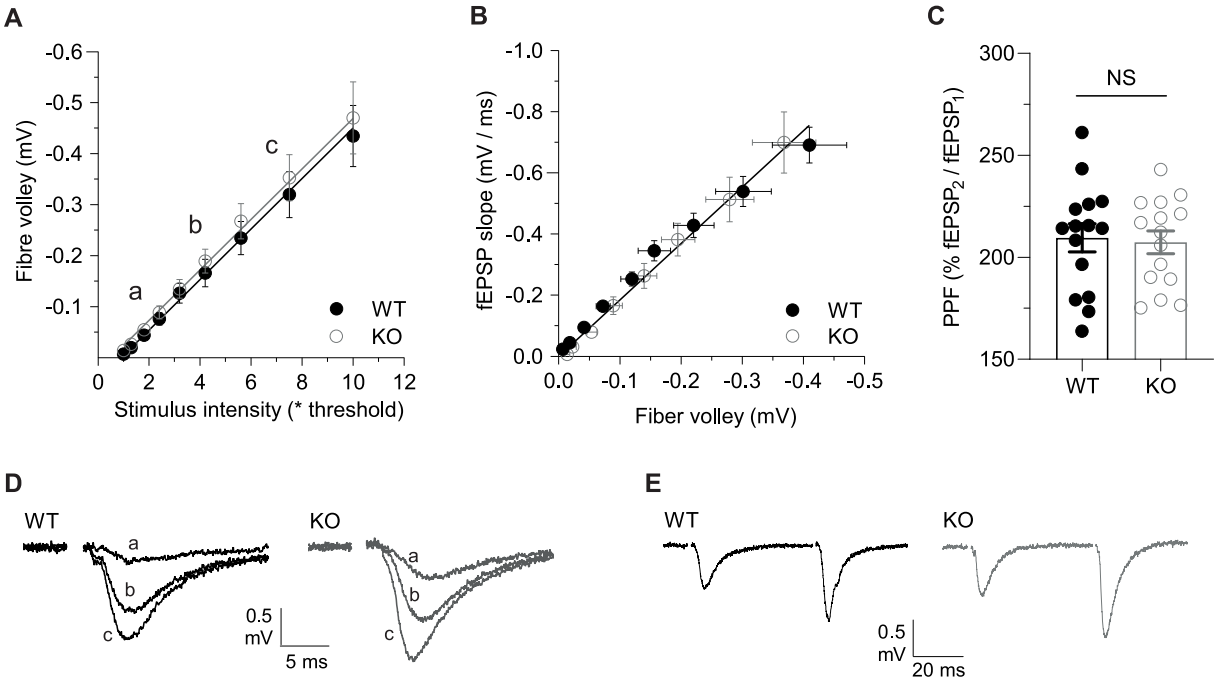

Fig. 1. Comparison of baseline synaptic transmission and PPF of WTs and GluN2D KOs.
(A) FV amplitude plotted against stimulus intensity. Slopes of WT line (−0.048 mV/stim intensity, n = 14) and KO line (−0.051 mV/stim intensity, n = 13) were not significantly different ($F(1, 239) = 0.5774$, $p = 0.448$, F test). **(B)** fEPSP to FV relationship for WT (slope of line = 1.8 ms^{-1}, n = 15) and KO (slope of line = 1.9 ms^{-1}, n = 11) were not significantly different ($F(1, 15) = 0.9132$, $p = 0.3544$, F test). **(C)** PPF (50 ms inter-pulse interval) was not significantly different between WTs (2.1 ± 0.07, n = 15) and KOs (2.1 ± 0.06, n = 15, $t(28) = 0.2460$, $p = 0.8075$, *t*-test). **(D)** Representative fEPSP traces from points indicated in A. **(E)** Representative fEPSP traces showing PPF in WTs (black) and GluN2D KOs (grey).

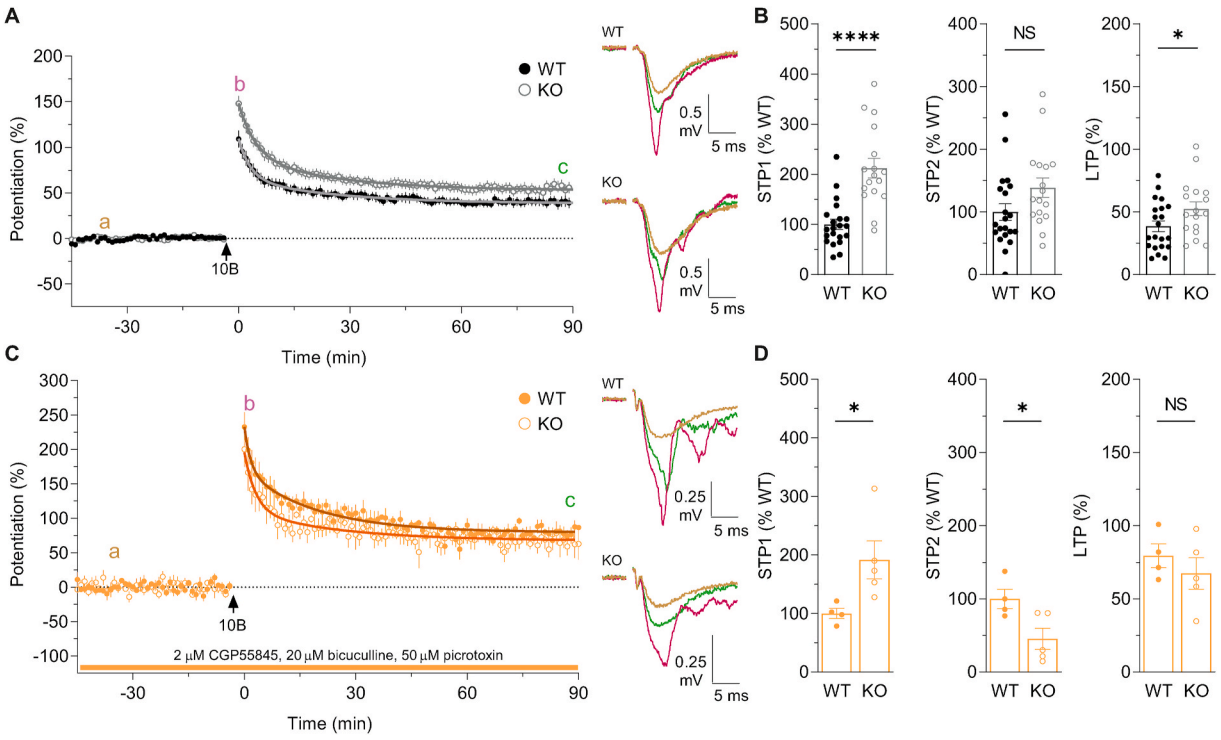

Fig. 2. *Altered synaptic plasticity in GluN2D KOs.*
(A) Pooled data showing the time course of potentiation of fEPSPs (mean ± SEM) for WTs (filled circles, n = 21) and KOs (open circles, n = 17). Decay of STP was fitted using a bi-exponential decay function (black curve fits WT and grey curve fits KO). The rate of decay of STP1 and STP2 were not significantly different between WTs (τ_1 = 3.0 min, τ2 = 24.0 min) and KOs (τ_1 = 4.7 min, τ2 = 25.8 min) (τ_1 F(1, 3333) = 1.231, p = 0.267, τ_2 F(1, 3333) = 0.0801, p = 0.777, F test). In this and subsequent time course plots, the arrowhead indicates the time of high frequency stimulation and the associated "B" refers to the number of bursts delivered. Representative fEPSPs from WTs and KOs at the time-points indicated in A are shown on the right. **(B)** The level of STP1 and STP2 were calculated by integrating the fast and slow components of the bi-exponential decay function, respectively, and are presented normalised with respect to the corresponding control. STP1 was significantly lower in WTs (100.0 ± 10.1%) compared to KOs (212.4 ± 19.4%; ****p < 0.0001, t(36) = 5.431, *t*-test). STP2 was not significantly different between WTs (100.0 ± 13.0%) and KOs (138.7 ± 15.7%; p = 0.0633, t(36) = 1.916, *t*-test). LTP in WTs (38.5 ± 4.3%) was significantly less than in KOs (52.5 ± 5.5%; t(36) = 2.055, *p = 0.0472, *t*-test) **(C)** Time course of potentiation in WTs (filled circles, n = 4) and KOs (open circles, n = 5) in the presence of $GABA_A$ and $GABA_B$ receptor antagonists. Decay time constant of STP1 and STP2 were not different between WTs (τ_1 = 1.7 min, τ_2 = 19.2 min) and KOs (τ_1 = 2.1 min, τ_2 = 25.1 min; τ_1 F(1, 796) = 1.081, p = 0.299; τ_2 F(1, 796) = 1.172, p = 0.279, F test). In this and subsequent figures, horizontal bars on the time course plots indicates the duration of compound application. **(D)** STP1 level was significantly lower in WT (100 ± 8.8%) compared to KOs (191.6 ± 32.2%; *p = 0.0437, t(7) = 2.456, *t*-test). STP2 was significantly greater in WTs (100 ± 13.4%) compared to KOs (45.5 ± 14.5%; *p = 0.0309, t(7) = 2.694, *t*-test). LTP was similar in WTs (79.4 ± 8.1%) and KOs (67.4 ± 10.7%; t(7) = 0.8548, p = 0.421; *t*-test).

(54.5 ± 14.5% decrease; Fig. 2D).

3.3. Sensitivity of STP and LTP to NMDAR antagonists

These data are consistent with an enhanced NMDAR-mediated LTP due to a reduction in feed-forward inhibition in the KOs, since GABAR-mediated inhibition limits the induction of LTP by intensifying the Mg^{2+} block of NMDARs (Wigström and Gustafsson, 1985; Herron et al., 1985; Dingledine et al., 1986). An alternative possibility is that constitutive absence of GluN2D subunits has resulted in the appearance of an additional NMDAR-independent form of LTP, which co-exists with NMDAR-dependent LTP (e.g., Jia et al., 1996). To test the NMDAR dependence of LTP we used a competitive antagonist, D-AP5, and a glycine-site antagonist, L-689,560, in both WTs (Fig. 3A and B) and KOs (Fig. 3C and D). In both genotypes, both D-AP5 and L-689,560 eliminated LTP (Fig. 3B, D). STP was also largely inhibited, though with D-AP5 a residual STP remained (Fig. 3B, D), which is consistent with the lower sensitivity of STP2 to this competitive antagonist (Volianskis et al., 2013a; Pradier et al., 2018).

3.4. UBP145 inhibits LTP in WTs but not KOs

In a previous study we found that, at a concentration of 10 μM, UBP145 did not significantly affect LTP (Volianskis et al., 2013a). We tested the same concentration of UBP145 on synaptic plasticity in WTs and KOs. To our surprise, UBP145 inhibited LTP by ~50% in WTs (from 47.5 ± 8.3% to 23.1 ± 6.5%; Fig. 4A and B). In contrast, UBP145 had no significant effect in KOs, consistent with its actions being selective for GluN2D-containing NMDARs (Fig. 4C and D). In contrast to the effect on LTP, UBP145 did not significantly affect STP1 or STP2, although there was a trend towards inhibition of STP2 in WTs (Fig. 4A and B).

3.5. Increasing the number of bursts alters STP and LTP in a GluN2D-dependent manner

We wondered if the lack of a significant effect of UBP145 on STP2, which contrasts with our previous observations in rats (Volianskis et al., 2013a; France et al., 2017), may be due to the lower level of STP2 in the present study and its overlap with LTP. Previous studies have shown that the GluN2D-selective NMDAR antagonist UBP145 inhibits a larger component of STP when 30-bursts (30B; Ingram et al., 2018) compared to when 10-bursts (10B; Volianskis et al., 2013a) are delivered in rats. This suggests that the contribution of STP2 to the total potentiation may be dependent on the number of stimuli during the induction phase. We therefore directly compared the effects of 10B (40 stimuli) and 30B (120 stimuli) in WTs (Fig. 5A and B) and assessed the dependence of any effects on GluN2D in KOs (Fig. 5C and D). In WTs, increasing from 10B to 30B increased LTP by ~80% (from 38.5 ± 4.3% to 68.6 ± 8.0%). In

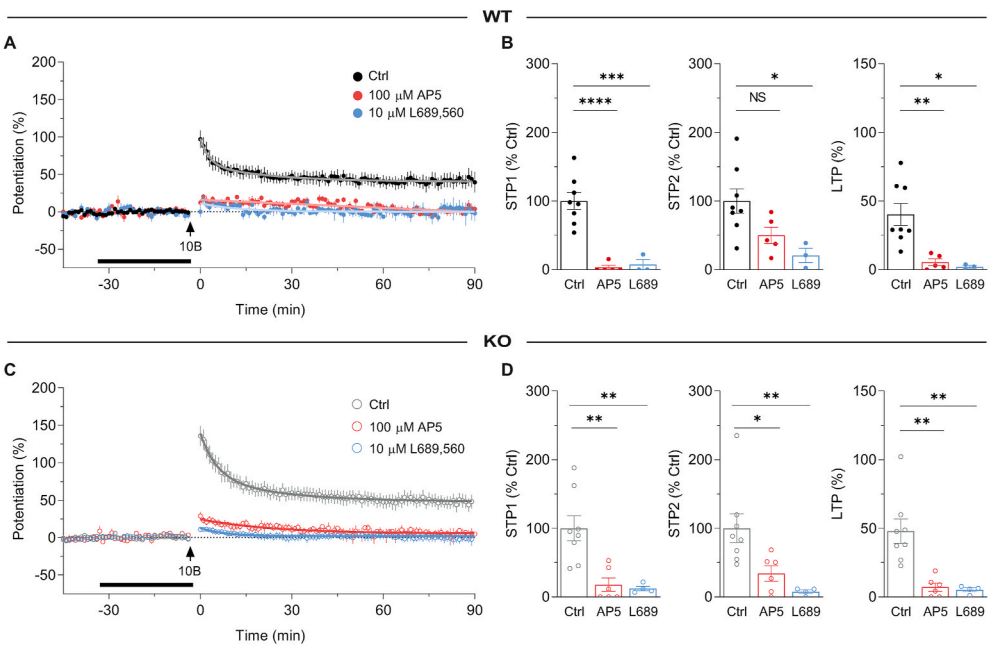

Fig. 3. Enhanced STP and LTP in GluN2D KOs is NMDAR-dependent.
(A) Time course of STP and LTP by 10-bursts in WTs. Data from control experiments (Ctrl, black circles, n = 8), 100 μM D-AP5 (red circles, n = 5) and 10 μM L-689,560 (blue circles, n = 3) are shown. **(B)** Summary of STP1, STP2 and LTP in WTs (from experiments shown in A) from control (STP1 = 100.0 ± 12.3%, STP2 = 100.0 ± 17.5%, LTP = 40.2 ± 8.0%), D-AP5 (STP1 = 3.1 ± 3.1%, STP2 = 50.3 ± 12.0%, LTP = 5.4 ± 2.4%) and L-689,560 (STP1 = 7.4 ± 7.4%, STP2 = 20.7 ± 10.5%, LTP = 2.0 ± 1.1%). STP1 was inhibited by D-AP5 (t(13) = 6.475, ****p < 0.0001, ANOVA with Bonferroni test for multiple comparisons (BT)) and L-689,560 (t(13) = 5.208, ***p = 0.0003, ANOVA with BT). STP2 was not significantly different in the D-AP5 (t(13) = 2.193, p = 0.0941, ANOVA) group but was significantly reduced in L-689,560 (t(13) = 2.945, *p = 0.0227, ANOVA with BT), compared to control. LTP was inhibited by D-AP5 (t(13) = 3.607, **p = 0.0064, ANOVA with BT) and L-689,560 (t(13) = 3.332, *p = 0.0108, ANOVA with BT). **(C)** Similar to A, but data are from KOs. Interleaved controls (grey circles, n = 8), D-AP5 (red circles, n = 6), and L-689,560 (blue circles, n = 4). **(D)** Summary of STP and LTP in KOs (from experiments shown in C) from control (STP1 = 100.0 ± 18.2%, STP2 = 100.0 ± 21.1%, LTP = 47.9 ± 8.8%), D-AP5 (STP1 = 17.9 ± 9.8%, STP2 = 34.1 ± 11.0%, LTP = 7.1 ± 3.0%) and L-689,560 (STP1 = 12.2 ± 3.3%, STP2 = 7.6 ± 2.7%, LTP = 5.2 ± 1.4%) experiments. STP1 was inhibited by D-AP5 (t(15) = 4.003, **p = 0.0023, ANOVA with BT) and L-689,560 (t(15) = 3.776, **p = 0.0037, ANOVA with BT). STP2 was inhibited by D-AP5 (t(15) = 2.791, *p = 0.0274, ANOVA with BT) and L-689,560 (t(10) = 3.451, **p = 0.007, ANOVA with BT), compared to control. LTP was inhibited by D-AP5 (t(15) = 4.280, **p = 0.0013, ANOVA with BT) and L-689,560 (t(15) = 3.956, **p = 0.0025, ANOVA with BT) compared to control.

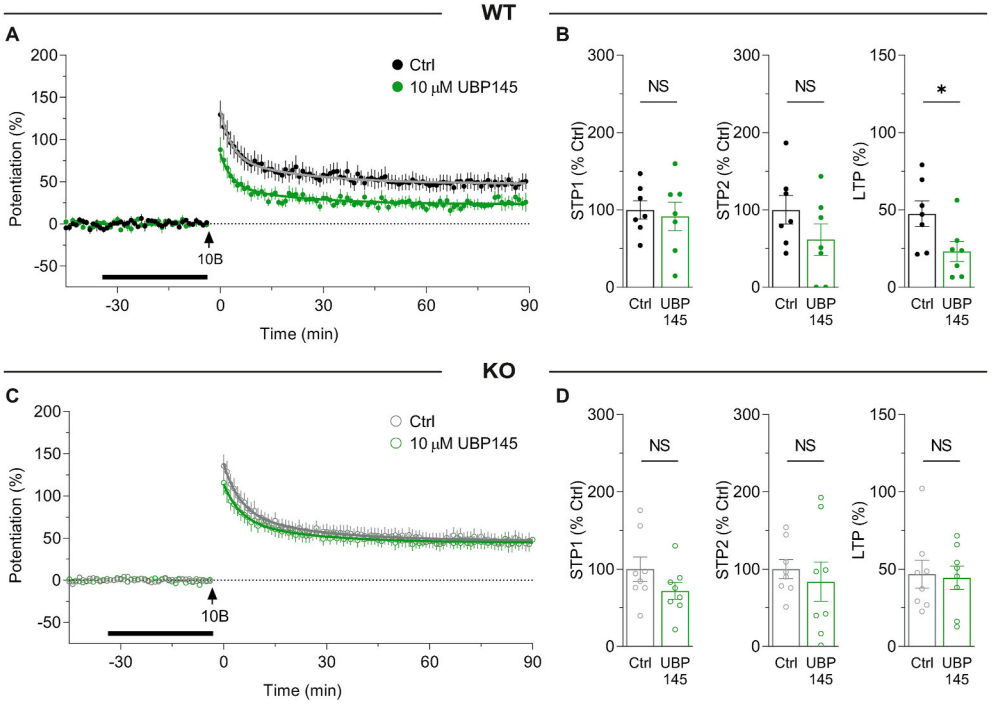

Fig. 4. UBP145 partially inhibits LTP in WTs but has no effect in GluN2D KOs.
(A) Time course of potentiation induced by 10-bursts in the presence of GluN2D antagonist 10 μM UBP145 (green circles, n = 7) compared to controls (black circles, n = 7) in WTs. **(B)** Summary of STP1, STP2 and LTP in WTs (from experiments shown in A) in control (STP1 = 100.0 ± 12.0%, STP2 = 100.0 ± 18.4%, LTP = 47.5 ± 8.3%) and UBP145 experiments (STP1 = 91.6 ± 18.4%, STP2 = 61.6 ± 20.3%, LTP = 23.1 ± 6.5%) in WTs. STP1 was not significantly different between the control and UBP145 groups (t(12) = 0.3813, p = 0.7096, *t*-test). STP2 was not significantly different between control and UBP145 (t(12) = 1.401, p = 0.1864, *t*-test). LTP was significantly reduced in UBP145-treated group compared to control (t(12) = 2.314, *p = 0.0392, *t*-test). **(C)** GluN2D KOs treated with UBP145 (green circles, n = 8) and controls (grey circles, n = 8). **(D)** Summary of potentiation in control (STP1 = 100.0 ± 15.8%, STP2 = 100.0 ± 12.4%, LTP = 46.8 ± 9.1%) and UBP145 experiments (STP1 = 71.8 ± 11.1%, STP2 = 83.8 ± 25.6%, LTP = 44.4 ± 7.5%) in KOs. STP1, STP2 and LTP were not significantly different between the control and UBP145 groups in KOs (STP1: t(14) = 1.458, p = 0.1668, *t*-test; STP2: t(14) = 0.5712, p = 0.5769, *t*-test; LTP: t(14) = 0.2077, p = 0.8384, *t*-test).

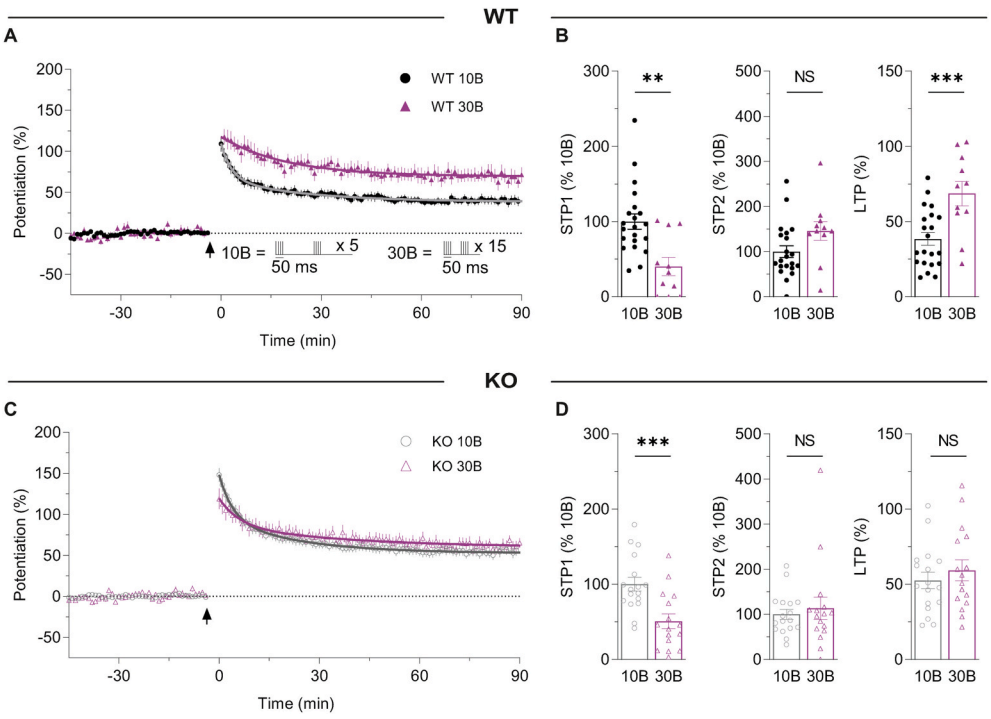

Fig. 5. Increasing burst number alters the STP and LTP profiles.
(A) Potentiation induced by 10-bursts (10B; black symbols, n = 21) and 30-bursts (30B; purple symbols, n = 11) in WTs. STP1 decay time constant (τ_1) values were similar in the 10-bursts (3.0 min) and 30-bursts (6.1 min) groups (F(1, 3319) = 0.0955, p = 0.7574, F test). τ_2 values were similar in 10-bursts (24.0 min) and 30-bursts (22.0 min) groups, in WTs (F(1, 3319) = 0.0897, p = 0.7646). **(B)** STP1 was significantly greater in the 10-bursts (100.0 ± 10.1%) compared to 30-bursts group (40.3 ± 12.1%; t(30) = 3.616, **p = 0.0011, *t*-test). STP2 was not significantly different between the groups receiving 10 bursts (100.0 ± 13.0%) and 30 bursts (145.5 ± 21.0%; t(30) = 1.934, p = 0.0620, *t*-test) groups. Total LTP was significantly increased in the 30-bursts group (68.6 ± 8.0%) compared to the 10-bursts group (38.5 ± 4.3%; t(30) = 3.6572, ***p = 0.0010, *t*-test) in WTs. **(C)** Equivalent data from KOs showing the time course of potentiation when induced with 10-bursts (black symbols, n = 17) and 30-bursts (purple symbols, n = 16). τ_1 and τ_2 were similar in 10-bursts (τ_1 = 4.7 min and τ_2 = 25.8 min) and 30-bursts (τ_1 = 5.2 min and τ_2 = 35.4 min) groups (for τ_1, F(1, 2947) = 0.0149, p = 0.9028; for τ_2, F(1, 2947) = 0.8230, p = 0.3644). **(D)** STP1 was significantly greater in the 10-bursts (100.0 ± 9.1%) group compared to 30-bursts (50.7 ± 9.7%; t(31) = 3.718, ***p = 0.0008, *t*-test). STP2 was not significantly different between the 10-bursts (100.0 ± 11.3%) and 30-bursts (113.4 ± 24.6%; t(31) = 0.5034, p = 0.6182, *t*-test) groups. LTP was similar in the 10-bursts group (52.5 ± 5.4%) and 30-bursts group (59.3 ± 6.9%; t(31) = 0.776, p = 0.4437, *t*-test).

contrast, STP1 was dramatically reduced by ~60% (from 100.0 ± 10.1% to 40.3 ± 12.1%). There was a trend towards higher STP2 of ~45% (from 100.0 ± 13.0% to 145.5 ± 21.0%; p = 0.0620, Fig. 5A and B). In the KOs, both LTP and STP2 were similar between the two induction protocols (Fig. 5C and D). In contrast, STP1 was significantly reduced by ~50% (from 100.0 ± 9.1% to 50.7 ± 9.7%). The decay time constants of

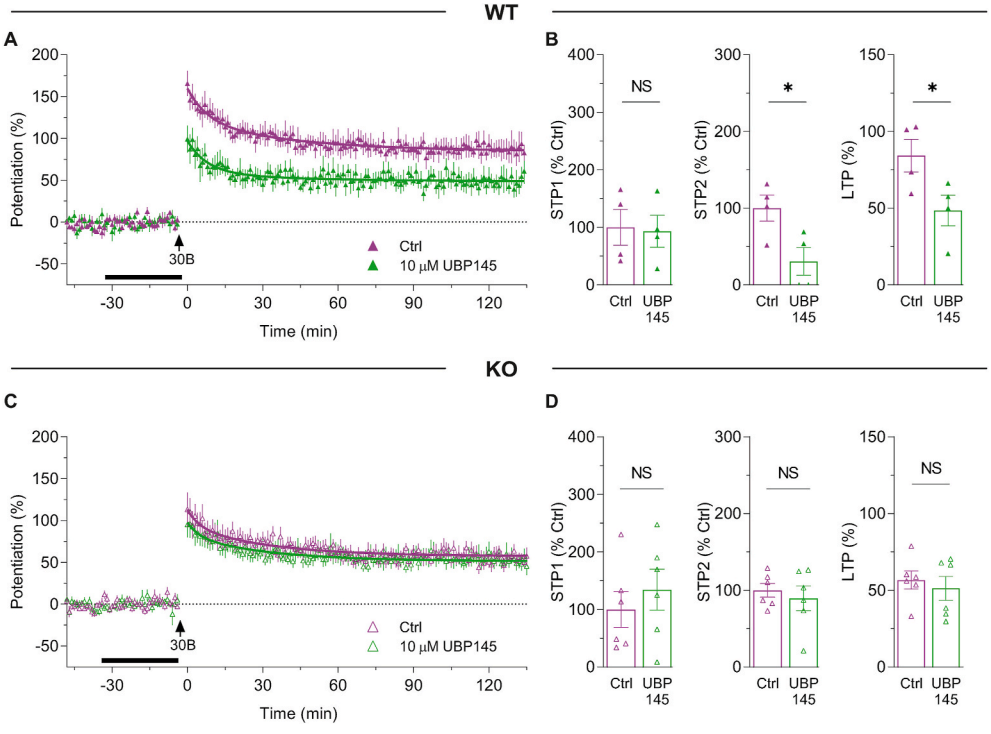

Fig. 6. The GluN2D subunit contributes to STP2 and LTP.
(A) Time course of potentiation in WTs induced by 30B in controls (purple symbols, n = 4), or in the presence of 10 μM UBP145 (green symbols, n = 4). **(B)** Summary of STP1, STP2 and LTP in WTs (from experiments shown in A) in control (STP1 = 100.0 ± 31.0%, STP2 = 100.0 ± 17.2%, LTP = 84.3 ± 10.7%) and UBP145 (STP1 = 92.9 ± 27.8%, STP2 = 30.6 ± 18.0%, LTP = 48.5 ± 10.0%) experiments in WTs. STP1 was not significantly different in UBP145 (t(6) = 0.1719, p = 0.8692, *t*-test) compared to control. STP2 was significantly lower in UBP145 (t(6) = 2.793, *p = 0.0315, *t*-test). LTP was partially inhibited by UBP145 (t(6) = 3.405, *p = 0.0144, *t*-test). **(C)** Equivalent data from KOs. Potentiation of control KOs (purple symbols, n = 6), UBP145 (green symbols, n = 6). **(D)** Summary of potentiation in control (STP1 = 100.0 ± 31.0%, STP2 = 100.0 ± 9.0%, LTP = 56.8 ± 6.0%), UBP145 (STP1 = 134.4 ± 35.4%, STP2 = 89.4 ± 16.0%, LTP = 51.3 ± 7.7%). STP1, STP2 and LTP were not significantly different upon treatment with UBP145 (STP1: t(10) = 0.732, p = 0.4811, STP2: t(10) = 0.575, p = 0.5781, LTP t(10) = 0.561, p = 0.5869, *t*-test).

STP1 and STP2 were not different between 10B and 30B in WTs or KOs (Fig. 5A, C).

3.6. UBP145 inhibits LTP and STP2 in WTs but not KOs

We next investigated the effects of UBP145 using the 30B protocol. In WTs, UBP145 significantly inhibited LTP by ~40% (from 84.3 ± 10.7% to 48.5 ± 10.0%) and STP2 by ~70% (from 100.0 ± 17.2% to 30.6 ± 18.0%; Fig. 6A and B). However, STP1 was not affected by UBP145 in WTs (Fig. 6A and B). In contrast to WTs, UBP145 had no effect in KOs on STP1, STP2 or LTP (Fig. 6C and D).

3.7. UBP145 inhibits NMDAR-EPSCs in neurons from WTs but not KOs

Finally, we examined the ability of 10 μM UBP145 to inhibit NMDAR-EPSCs (Fig. 7). In CA1 pyramidal neurons, UBP145 inhibited the EPSC amplitude by 38.4 ± 2.6% (Fig. 7A and B), which is similar to our previous observations in rats (IC_{50} = 11.5 μM; Volianskis et al., 2013a). In *stratum radiatum* interneurons (SR IN) we also observed a substantial inhibition of the NMDAR-EPSC in WTs (40.5 ± 3.1%) but there was no effect in KOs (−5.9 ± 2.4%; Fig. 7C and D). We conclude therefore that the inhibition of NMDAR-EPSCs by 10 μM UBP145 is mediated by an action on GluN2D-containing NMDARs and that there is no appreciable difference between rats and mice in this action.

4. Discussion

In the present study we have combined the use of UBP145, a GluN2C/D antagonist, and a GluN2D KO mouse line to investigate the role of GluN2D-containing NMDARs in synaptic plasticity in the CA1 region of mouse hippocampal slices. We made several original observations: (i) we found that LTP is enhanced in the KOs when we used a comparatively weak induction protocol, comprising of 40 stimuli. (ii) This difference between genotypes was not observed when we either blocked GABA receptor-mediated inhibition or increased the number of stimuli three-fold. (iii) We found that UBP145 inhibits LTP in WTs but not KOs. (iv) With respect to STP, increasing the number of stimuli during the induction results in less STP1 in both WTs and KOs. (v) STP2 is inhibited by UBP145 in WTs but not KOs. These data indicate the complex role of GluN2D-containing NMDARs in hippocampal synaptic plasticity.

4.1. Multiple forms of NMDAR-dependent synaptic plasticity

In the present study we have investigated three forms of NMDAR-dependent synaptic plasticity – STP1, STP2 and LTP. Note that there are several additional forms of NMDAR-dependent synaptic plasticity that were not triggered by the stimulus parameters used; these include an additional, mechanistically distinct form of LTP, which requires spaced episodes of TBS and involves PKA, calcium-permeable AMPARs and *de novo* protein synthesis (see Park et al., 2016, 2021) as well as *de novo* LTD and depotentiation, both of which require lower frequencies of stimulation for their induction (see Collingridge et al., 2010). However, even by restricting our analysis to three components of synaptic plasticity the situation is complex, due to the temporal overlap of STP1, STP2 and LTP. To quantify STP1 and STP2 we integrated the area under their respective decays on the assumption that LTP has reached a steady state level at 4 min post TBS. Due to the presence of STP, it is not possible to know the precise time-course of the generation of LTP, though it may develop gradually over several minutes under the present recording

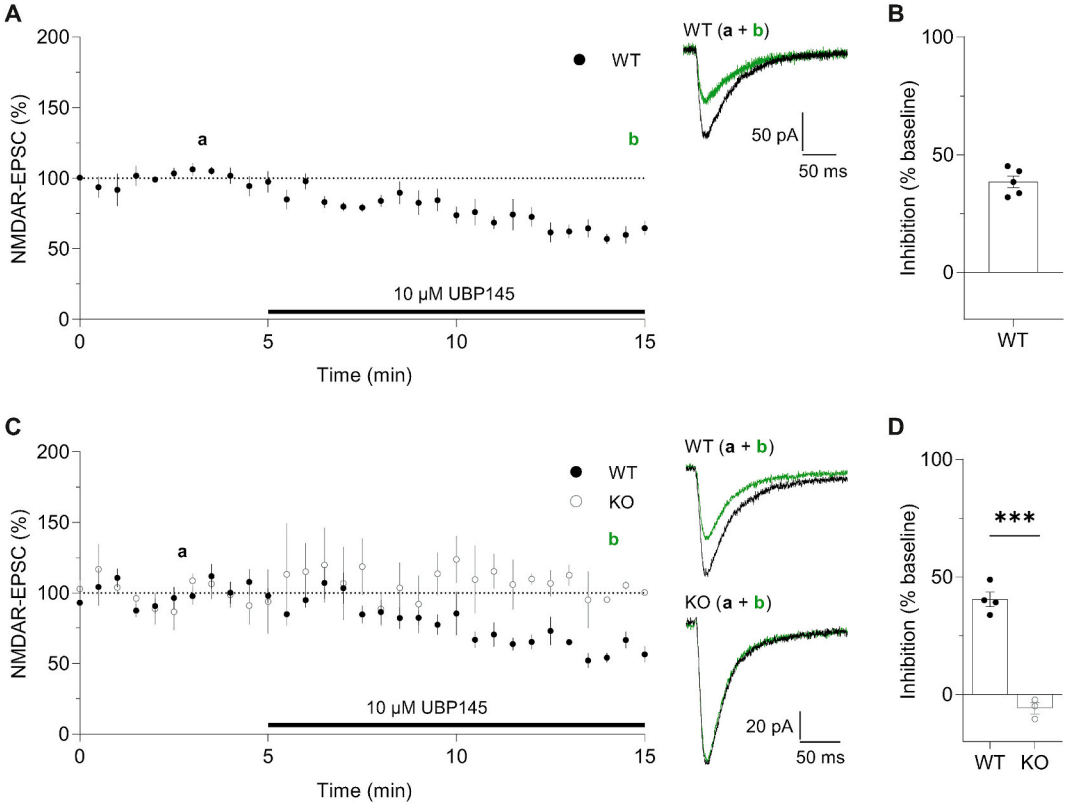

Fig. 7. UBP145 inhibits NMDAR-mediated EPSCs from CA1 pyramidal cell and SR IN in WTs.
(A) NMDAR EPSCs from CA1 pyramidal cells in WTs (n = 5). Representative traces (right) showing NMDAR EPSCs from baseline period (**a**) and at the end of UBP145 application (**b**) **(B)** UBP145 (10 μM) inhibited NDMAR EPSCs by 38.4 ± 2.6%. **(C)** Similar to panel A but NMDAR EPSCs from SR IN in WTs (closed circles, n = 4) and KOs (open circles, n = 3). **(D)** NMDAR EPSC from SR IN was significantly inhibited by 10 μM UBP145 in WTs (40.5 ± 3.1%) but not KOs (−5.9 ± 2.4%; ***p = 0.0001, t(5) = 11.06, *t*-test).

conditions (Davies et al., 1989). In which case, the area calculations would be slight underestimates, particularly for STP1. Since STP2 decays with a time-constant of ~25 min, it will not appreciably affect the estimate of LTP measured ~90 min following its induction. Another form of synaptic plasticity at these synapses is post-tetanic potentiation (PTP), that decays rapidly within a couple of minutes and is NMDAR independent. We avoided any contamination of the STP measurement by pausing stimulation for 3 min immediately following the termination of the TBS, since PTP decays passively whereas STP only decays in response to activity (Volianskis and Jensen, 2003).

4.2. Role of GluN2D-containing NMDARs in the induction of LTP

When we examined the effects of UBP145 on LTP in rat hippocampal slices we observed inhibition, but only at concentrations above 10 μM that affected GluN2A- and GluN2B-containing NMDARs (Volianskis et al., 2013a). We reasoned that LTP was mediated by GluN2A- and GluN2B-containing NMDARs, primarily in the form of a GluN1/-GluN1/GluN2A/GluN2B triheteromer (Volianskis et al., 2013a). In contrast, in the present study, 10 μM UBP145 produced a substantial inhibition of LTP (Fig. 4). Since UBP145 had no effect on LTP in the KOs, we can conclude that its effects were mediated via GluN2D-containing NMDARs. The differing effectiveness of UBP145 against LTP in rats *vs* mice may be a species difference. Differences between species or even within strains can profoundly affect glutamatergic synaptic function; for example some Wistar rats have an endogenous KO of the mGlu2 receptor (Ceolin et al., 2011). Arguing against a species difference we observed similar inhibition of NMDAR-EPSCs in mice in the present study as we reported previously in rats (Volianskis et al., 2013a). However, it is possible that the level of inhibition of the NMDAR-EPSC required to affect LTP is different between mice and rats.

The finding that LTP was moderately enhanced in the KO was surprising, particularly in light of the opposite effects of the antagonist. Since the difference between WT and KO was absent when GABA receptor-mediated inhibition was blocked, it seems likely that the absence of GluN2D results in a weaker excitatory drive of feedforward inhibitory interneurons. Consistent with this possibility, GluN2D-containing NMDARs are known to contribute to the excitation of GABA interneurons in area CA1 of the hippocampus (Perszyk et al., 2016; Swanger et al., 2018; Yi et al., 2019). Pharmacological antagonism of synaptic inhibition promotes the synaptic activation of NMDARs (Herron et al., 1985; Dingledine et al., 1986) and can facilitate the induction of LTP (Wigström and Gustafsson, 1985). Furthermore, the principle that reducing the excitatory drive of feedforward interneurons can promote the induction of LTP has already been demonstrated using GluK1 antagonists (Clarke et al., 2012). The facilitation of LTP observed in the KO was not observed when the stronger induction protocol was used. This is consistent with the proposal that the facilitation of LTP in the KO, observed with the weaker induction protocol, is due to an effect via synaptic inhibition. Mechanisms that regulate the induction of LTP via affecting synaptic inhibition are negated not only by GABA receptor antagonists but also by using stronger induction protocols, due to frequency-dependent changes in synaptic inhibition (Davies and Collingridge, 1996).

Although LTP is usually assessed by measuring AMPAR-mediated synaptic transmission, it is also possible to observe LTP of NMDAR-mediated synaptic transmission (Bashir et al., 1991; Berretta et al., 1991). Interestingly, Anwyl and colleagues showed, using PPDA and UBP141, that the expression of LTP of NMDAR-mediated synaptic transmission in the dentate gyrus is due to the synaptic incorporation of GluN2D-containing NMDARs from extrasynaptic sites (Harney et al., 2008). At stellate synapses in the cerebellum it has been shown, using the GluN2D KO and pharmacological agents including PPDA, that presynaptic GluN2B/D triheteromers trigger the persistent increase in GABA release (Dubois et al., 2016).

In conclusion, studies using GluN2C/D antagonists from the Bristol laboratory, sometimes in conjunction with the GluN2D KO mouse line, have uncovered complex roles of GluN2D-containing NMDARs in various forms of synaptic plasticity. Our present study has shown how GluN2D-containing NMDARs can both contribute to and serve to limit the induction of LTP at CA1 synapses in the hippocampus.

4.3. Role of GluN2D-containing NMDARs in STP

We previously reported that UBP145 inhibited a slow component of STP, which we termed STP2, without affecting a fast component (STP1) or LTP in slices from either adult (Volianskis et al., 2013a) or juvenile rats (France et al., 2017). In the present study, we also observed inhibition of STP2, defined by its slow time-constant of decay, by UBP145, which is entirely consistent with the previous results in rats. To observe a significant effect of UBP145 on STP2, it was necessary to use the 30B protocol. We attribute the lack of effect of UBP145 in the 10B protocol to the relatively small contribution of STP2 to the total synaptic potentiation and the masking effect of the indirect facilitation of LTP. UBP145 does not distinguish between GluN2C and GluN2D (Costa et al., 2009). GluN2C-containing NMDARs are expressed in astrocytes (Ravikrishnan et al., 2018; Alsaad et al., 2019) where they could, in principle, orchestrate STP2. However, the lack of effect of UBP145 in the GluN2D KO makes this scenario extremely unlikely. It is also important to note that STP2, unlike STP1 and LTP, is also sensitive to low concentrations of GluN2B antagonists, suggesting that the receptor responsible for STP2 is a GluN2B/D-containing triheteromer (Volianskis et al., 2013a), a native subunit configuration (e.g., Brickley et al., 2003) that, unlike GluN2A/2B triheteromers, has high sensitivity to GluN2B antagonists, such as ifenprodil (Yi et al., 2019).

Where are the GluN2D-containing NMDARs that mediate STP2 located? In our experiments STP, but not LTP, is consistently associated with a decrease in PPF, indicative of an increase in probability of neurotransmitter release (P(r)) (Volianskis and Jensen, 2003; Volianskis et al., 2013b). Although PPF may, under certain circumstances, be due to a postsynaptic alteration (e.g., Wang and Kelly, 1997) and that in some laboratories STP has been observed without a change in PPF (e.g., Schulz and Fitzgibbons, 1997) we base our hypotheses on a presynaptic mechanism. Our initial study observed that NMDA profoundly affected the presynaptic fibre volley (Collingridge et al., 1983), which is indicative of presynaptic NMDARs at SC-CA1 synapses. Although a postsynaptic mechanism for this effect could not be excluded, subsequent work provided direct pharmacological support for the existence of presynaptic NMDARs in the entorhinal cortex (Berretta and Jones, 1996). More recently, the regulation of L-glutamate release at SC-CA1 synapses has been observed directly (McGuinness et al., 2010). We suspect therefore that STP2 is generated by the actions of synaptically released L-glutamate on GluN2B/GluN2D triheteromers to enhance L-glutamate release. It is noteworthy that this NMDAR subtype has been found to regulate neurotransmitter release at other synapses (Dubois et al., 2016).

The present findings have uncovered an interesting relationship between STP1 and STP2. We found that as we increased the burst number (from 10 to 30), there was a trend towards greater STP2 magnitude and a significant reduction of STP1 (Fig. 5B). This may be due to convergence on a common presynaptic mechanism that increases P(r). How these two processes are engaged by different NMDAR subtypes and why they have different decay kinetics remains a matter of speculation. One possibility that we have considered is that STP1 is generated by the activation of the same postsynaptic GluN2A/B triheteromers that trigger LTP, since STP1 has a similar pharmacology as LTP (Volianskis et al., 2013a). Potassium efflux from NMDARs could directly depolarise adjacent presynaptic terminals to trigger STP1. Previously, we proposed that K^+ efflux from postsynaptic NMDARs may signal to local presynaptic terminals (Collingridge, 1992) and experimental support for this idea has since been obtained (Shih et al., 2013). In contrast, STP2 may be triggered by synaptically released L-glutamate acting upon

presynaptic GluN2B/D triheteromers. But this leaves the question as to why some synapses utilise the first mechanism and some the second? Again, we can only speculate but one possibility is that this relates to the basal P(r) of the synapses, which is known to be both highly variable at these synapses and dominated by low P(r) synapses (see Sanderson et al., 2018). Potentially, high P(r) synapses may engage STP1 and low P(r) synapses may engage STP2. Accordingly, 120 stimuli (during 30B) will engage considerably more synapses than 40 stimuli (during 10B). In other words, increasing the number of stimuli during induction may increase the STP2 component by recruiting more low P(r) synapses, via presynaptic GluN2B/D-containing triheteromers.

This process may also explain the different decay kinetics of STP1 and STP2. Both STP1 and STP2 are stored in time until there is a stimulus, at which point the response starts to decline with each stimulus (Volianskis et al., 2013a). It seems plausible that at the level of individual synapses either STP1 or STP2 primes the synapse to increase its P(r) for the next release event, at which point the release probability is reset to the basal level. In which case, STP will decline according to the basal P(r); in other words, high P(r) synapses will be reset more quickly than low P(r) synapses resulting in more rapid decay kinetics. This leaves a couple more questions: firstly, why with the 30B train was there less STP1? It seems plausible that high P(r) synapses are both primed and reset during the 120 stimuli that constitute the 30B train. Consistent with this scenario, increasing the number of bursts resulted in significantly less STP1 in the KOs. Secondly, why does postsynaptic activation of GluN2A/2B only induce STP at high P(r) synapses (i.e., STP1) and not at low P(r) synapses (i.e., STP2)? Perhaps at high P(r) synapses there is sufficient temporal activity to bypass the need for the presynaptic GluN2B/2D triheteromers, whereas at low P(r) synapses, with their sparse activation, these presynaptic NMDARs are a requirement. This would fit with a model where the point of convergence is at the level of presynaptic Ca^{2+} signalling. To address these mechanisms directly it will be necessary to record Ca^{2+} activity within presynaptic boutons (McGuinness et al., 2010) and relate this to their P(r) (Sanderson et al., 2018).

Finally, it is worth noting that the present observations raise the possibility that activation of presynaptic GluN2D-containing NMDARs serves to facilitate the induction of LTP by increasing the probability of a release event occurring at low P(r) synapses during the induction protocol. If so, this could explain, at least in part, the reduction of LTP by UBP145. This would mean that the increase in P(r), orchestrated by the GluN2D-containing NMDARs, serves two purposes: one to transiently increase synaptic transmission in a way that alters the dynamic response of the neuron to high frequency bursts (Volianskis et al., 2013b) and the second to increase the probability of a Hebbian conjunction at low P(r) synapses during the induction, resulting in a larger LTP. Further work is required to dissect out the relative contributions of pre- and post-synaptic GluN2D-containing NMDARs to the induction of LTP.

4.4. Functions of GluN2D-containing NMDARs in health and disease

It is established that NMDAR-dependent LTP at SC-CA1 synapses is important for learning and memory (e.g., Morris et al., 1986). Accordingly, the present findings that GluN2D-containing NMDARs can contribute to LTP adds to the established roles of GluN2A- and GluN2B-containing NMDARs in hippocampus-dependent learning and memory. A role for GluN2D-containing NMDARs in extinction learning and cerebellar plasticity has been observed (Dubois and Liu, 2021). The function of STP is less well established but, as we have argued previously (Ingram et al., 2018), could be important for forms of short-term memory; in particular those where information has to be held in storage until accessed and then discarded. The role of GluN2D-containing NMDARs in the excitation of feedforward GABAergic interneurons, will also influence the induction of synaptic plasticity, as we have demonstrated here. Thus, GluN2D-containing NMDARs are likely to be important in cognitive processes in complex ways.

Dysregulation of GluN2D-containing NMDARs is also likely to be involved in a variety of disorders. GluN2D KO mice (Ikeda et al., 1995) possess a number of interesting phenotypes, such as lack of phencyclidine-induced hyperlocomotor activity (Hagino et al., 2010). This observation indicated that GluN2D may be an important site of action of the uncompetitive NMDAR channel blockers. This is supported by pharmacological data that shows that ketamine and memantine are more potent antagonists at GluN2C- and GluN2D- vs GluN2A- and GluN2B-containing NMDARs, in the presence of physiological concentrations of Mg^{2+} (Kotermanski and Johnson, 2009). These and other data suggest that GluN2D-containing NMDARs may be a therapeutic target for the actions of these drugs in the treatment of depression and dementia, respectively. In terms of depression, however, the GluN2D subunit may be more important for the effects of the *R*-enantiomer of ketamine (Ide et al., 2017). We have shown that STP2 is exquisitely sensitive to the actions of ketamine (Ingram et al., 2018), showing that native receptor configurations containing the GluN2D subunit are amongst the targets of low doses of ketamine. Altered function involving GluN2D-containing NMDARs may also be important in a variety of other serious disorders, including schizophrenia (Sapkota et al., 2016; Mao et al., 2020), excitotoxicity (Bai et al., 2013) and chronic pain (Temi et al., 2021). In this context, recent studies in the anterior cingulate cortex have shown, using UBP145 and PPDA, that GluN2D-containing NMDARs regulate the frequency of spontaneous synaptic events (Chen et al., 2021). Systemic administration of UBP141 was found to very effectively suppress seizures in a model of tuberous sclerosis, though this effect was attributed to antagonism of GluN2C-containing NMDARs (Lozovaya et al., 2014). In another study it was found that UBP145 protected against neurotoxicity that is promoted by tissue plasminogen activator (Jullienne et al., 2011). These experiments indicate the wide therapeutic potential of GluN2D (and GluN2C) antagonists. Understanding the physiological functions of GluN2D-containing NMDARs should help in elucidating how these receptors are involved in a variety of major pathological conditions.

4.5. Concluding remarks

By the combined use of a global GluN2D KO and UBP145, we have been able to identify several distinct functions of GluN2D-containing NMDARs in synaptic plasticity in mouse hippocampal slices. The availability of a variety of pharmacological tools, which include other competitive GluN2D antagonists (Wang et al., 2020) and allosteric modulators (Mullasseril et al., 2010; Swanger et al., 2018), along with constitutive and conditional GluN2D KOs should enable additional synaptic functions of these receptors to be identified. A mechanistic understanding of the role of GluN2D-containing NMDARs in synaptic plasticity is required to fully understand the role of these receptors in health and disease.

Acknowledgements

We are extremely grateful to Professor Masayoshi Mishina for providing the GluN2D KO mice. This work was supported by the MRC (UK) and CIHR (Canadian Institutes of Health Research, Foundation Grant #154276) grants to GLC. GLC is the holder of the Krembil Family Chair in Alzheimer's Research. Additional support came from "The Neuroscience Catalyst" research program of the Centre for Collaborative Drug Research (CCDR) at the University of Toronto (GLC and JG). Alen Eapen was a recipient of a SWBio Doctoral Training Partnership grant from Biotechnology and Biological Sciences Research Council (BBRC), UK.

References

Alsaad, H.A., DeKorver, N.W., Mao, Z., Dravid, S.M., Arikkath, J., Monaghan, D.T., 2019. In the telencephalon, GluN2C NMDA receptor subunit mRNA is predominately

expressed in glial cells and GluN2D mRNA in interneurons. Neurochem. Res. 44, 61–77.
Anderson, W., Collingridge, G., 2007. Capabilities of the WinLTP data acquisition program extending beyond basic LTP experimental functions. J. Neurosci. Methods 162, 346–356.
Bai, N., Hayashi, H., Aida, T., Namekata, K., Harada, T., Mishina, M., Tanaka, K., 2013. Dock3 interaction with a glutamate-receptor NR2D subunit protects neurons from excitotoxicity. Mol. Brain 6, 22.
Bartlett, T.E., Bannister, N.J., Collett, V.J., Dargan, S.L., Massey, P.V., Bortolotto, Z.A., Fitzjohn, S.M., Bashir, Z.I., Collingridge, G.L., Lodge, D., 2007. Differential roles of NR2A and NR2B-containing NMDA receptors in LTP and LTD in the CA1 region of two-week old rat hippocampus. Neuropharmacology 52, 60–70.
Bashir, Z.I., Alford, S., Davies, S.N., Randall, A.D., Collingridge, G.L., 1991. Long-term potentiation of NMDA receptor-mediated synaptic transmission in the hippocampus. Nature 349, 156–158.
Berretta, N., Berton, F., Bianchi, R., Brunelli, M., Capogna, M., Francesconi, W., 1991. Long-term potentiation of NMDA receptor-mediated EPSP in Guinea-pig hippocampal slices. Eur. J. Neurosci. 3, 850–854.
Berretta, N., Jones, R.S., 1996. Tonic facilitation of glutamate release by presynaptic N-methyl-D-aspartate autoreceptors in the entorhinal cortex. Neuroscience 75, 339–344.
Brickley, S.G., Misra, C., Mok, M.H.S., Mishina, M., Cull-Candy, S.G., 2003. NR2B and NR2D subunits coassemble in cerebellar Golgi cells to form a distinct NMDA receptor subtype restricted to extrasynaptic sites. J. Neurosci. 23, 4958–4966.
Ceolin, L., Kantamneni, S., Barker, G.R.I., Hanna, L., Murray, L., Warburton, E.C., Robinson, E.S.J., Monn, J.A., Fitzjohn, S.M., Collingridge, G.L., et al., 2011. Study of novel selective mGlu2 agonist in the temporo-ammonic input to CA1 neurons reveals reduced mGlu2 receptor expression in a Wistar substrain with an anxiety-like phenotype. J. Neurosci. 31, 6721–6731.
Chen, Q.-Y., Li, X.-H., Lu, J.-S., Liu, Y., Lee, J.-H.A., Chen, Y.-X., Shi, W., Fan, K., Zhuo, M., 2021. NMDA GluN2C/2D receptors contribute to synaptic regulation and plasticity in the anterior cingulate cortex of adult mice. Mol. Brain 14, 60.
Clarke, V.R.J., Collingridge, G.L., Lauri, S.E., Taira, T., 2012. Synaptic kainate receptors in CA1 interneurons gate the threshold of theta-frequency-induced long-term potentiation. J. Neurosci. 32, 18215–18226.
Collingridge, G.L., 1992. The Sharpey-Schafer Prize Lecture. The mechanism of induction of NMDA receptor-dependent long-term potentiation in the hippocampus. Exp. Physiol. 77, 771–797.
Collingridge, G.L., Kehl, S.J., McLennan, H., 1983. Excitatory amino acids in synaptic transmission in the Schaffer collateral-commissural pathway of the rat hippocampus. J. Physiol. 334, 33–46.
Collingridge, G.L., Olsen, R.W., Peters, J., Spedding, M., 2009. A nomenclature for ligand-gated ion channels. Neuropharmacology 56, 2–5.
Collingridge, G.L., Peineau, S., Howland, J.G., Wang, Y.T., 2010. Long-term depression in the CNS. Nat. Rev. Neurosci. 11, 459–473.
Costa, B.M., Feng, B., Tsintsadze, T.S., Morley, R.M., Irvine, M.W., Tsintsadze, V., Lozovaya, N.A., Jane, D.E., Monaghan, D.T., 2009. N-Methyl-d-aspartate (NMDA) receptor NR2 subunit selectivity of a series of novel piperazine-2,3-dicarboxylate derivatives: preferential blockade of extrasynaptic NMDA receptors in the rat hippocampal CA3-CA1 synapse. J. Pharmacol. Exp. Therapeut. 331, 618–626.
Davies, C.H., Collingridge, G.L., 1996. Regulation of EPSPs by the synaptic activation of GABAB autoreceptors in rat hippocampus. J. Physiol. 496 (Pt 2), 451–470.
Davies, J., Francis, A.A., Jones, A.W., Watkins, J.C., 1981. 2-Amino-5-phosphonovalerate (2APV), a potent and selective antagonist of amino acid-induced and synaptic excitation. Neurosci. Lett. 21, 77–81.
Davies, J., Evans, R.H., Herrling, P.L., Jones, A.W., Olverman, H.J., Pook, P., Watkins, J. C., 1986. CPP, a new potent and selective NMDA antagonist. Depression of central neuron responses, affinity for [3H]D-AP5 binding sites on brain membranes and anticonvulsant activity. Brain Res. 382, 169–173.
Davies, S.N., Lester, R.A.J., Reymann, K.G., Collingridge, G.L., 1989. Temporally distinct pre- and post-synaptic mechanisms maintain long-term potentiation. Nature 338, 500–503.
Dingledine, R., Hynes, M.A., King, G.L., 1986. Involvement of N-methyl-D-aspartate receptors in epileptiform bursting in the rat hippocampal slice. J. Physiol. (Lond.) 380, 175–189.
Dubois, C.J., Liu, S.J., 2021. GluN2D NMDA receptors gate fear extinction learning and interneuron plasticity. Front. Synaptic Neurosci. 13.
Dubois, C.J., Lachamp, P.M., Sun, L., Mishina, M., Liu, S.J., 2016. Presynaptic GluN2D receptors detect glutamate spillover and regulate cerebellar GABA release. J. Neurophysiol. 115, 271–285.
France, G., Fernández-Fernández, D., Burnell, E.S., Irvine, M.W., Monaghan, D.T., Jane, D.E., Bortolotto, Z.A., Collingridge, G.L., Volianskis, A., 2017. Multiple roles of GluN2B-containing NMDA receptors in synaptic plasticity in juvenile hippocampus. Neuropharmacology 112, 76–83.
Hagino, Y., Kasai, S., Han, W., Yamamoto, H., Nabeshima, T., Mishina, M., Ikeda, K., 2010. Essential role of NMDA receptor channel ε4 subunit (GluN2D) in the effects of phencyclidine, but not methamphetamine. PLoS One 5, e13722.
Harney, S.C., Jane, D.E., Anwyl, R., 2008. Extrasynaptic NR2D-containing NMDARs are recruited to the synapse during LTP of NMDAR-EPSCs. J. Neurosci. 28, 11685–11694.
Herron, C.E., Williamson, R., Collingridge, G.L., 1985. A selective N-methyl-D-aspartate antagonist depresses epileptiform activity in rat hippocampal slices. Neurosci. Lett. 61, 255–260.
Hrabetova, S., Serrano, P., Blace, N., Tse, H.W., Skifter, D.A., Jane, D.E., Monaghan, D.T., Sacktor, T.C., 2000. Distinct NMDA receptor subpopulations contribute to long-term potentiation and long-term depression induction. J. Neurosci. 20, RC81.
Ide, S., Ikekubo, Y., Mishina, M., Hashimoto, K., Ikeda, K., 2017. Role of NMDA receptor GluN2D subunit in the antidepressant effects of enantiomers of ketamine. J. Pharmacol. Sci. 135, 138–140.
Ikeda, K., Araki, K., Takayama, C., Inoue, Y., Yagi, T., Aizawa, S., Mishina, M., 1995. Reduced spontaneous activity of mice defective in the ε4 subunit of the NMDA receptor channel. Mol. Brain Res. 33, 61–71.
Ingram, R., Kang, H., Lightman, S., Jane, D.E., Bortolotto, Z.A., Collingridge, G.L., Lodge, D., Volianskis, A., 2018. Some distorted thoughts about ketamine as a psychedelic and a novel hypothesis based on NMDA receptor-mediated synaptic plasticity. Neuropharmacology 142, 30–40.
Irvine, M.W., Costa, B.M., Dlaboga, D., Culley, G.R., Hulse, R., Scholefield, C.L., Atlason, P., Fang, G., Eaves, R., Morley, R., et al., 2012. Piperazine-2,3-dicarboxylic acid derivatives as dual antagonists of NMDA and GluK1-containing kainate receptors. J. Med. Chem. 55, 327–341.
Jia, Z., Agopyan, N., Miu, P., Xiong, Z., Henderson, J., Gerlai, R., Taverna, F.A., Velumian, A., MacDonald, J., Carlen, P., et al., 1996. Enhanced LTP in mice deficient in the AMPA receptor GluR2. Neuron 17, 945–956.
Jullienne, A., Montagne, A., Orset, C., Lesept, F., Jane, D.E., Monaghan, D.T., Maubert, E., Vivien, D., Ali, C., 2011. Selective inhibition of GluN2D-containing N-methyl-D-aspartate receptors prevents tissue plasminogen activator-promoted neurotoxicity both in vitro and in vivo. Mol. Neurodegener. 6, 68.
Karp, S.J., Masu, M., Eki, T., Ozawa, K., Nakanishi, S., 1993. Molecular cloning and chromosomal localization of the key subunit of the human N-methyl-D-aspartate receptor. J. Biol. Chem. 268, 3728–3733.
Kotermanski, S.E., Johnson, J.W., 2009. Mg2+ imparts NMDA receptor subtype selectivity to the Alzheimer's drug memantine. J. Neurosci. 29, 2774–2779.
Kutsuwada, T., Kashiwabuchi, N., Mori, H., Sakimura, K., Kushiya, E., Araki, K., Meguro, H., Masaki, H., Kumanishi, T., Arakawa, M., 1992. Molecular diversity of the NMDA receptor channel. Nature 358, 36–41.
Liu, L., Wong, T.P., Pozza, M.F., Lingenhoehl, K., Wang, Y., Sheng, M., Auberson, Y.P., Wang, Y.T., 2004. Role of NMDA receptor subtypes in governing the direction of hippocampal synaptic plasticity. Science 304, 1021–1024.
Lozovaya, N., Gataullina, S., Tsintsadze, T., Tsintsadze, V., Pallesi-Pocachard, E., Minlebaev, M., Goriounova, N.A., Buhler, E., Watrin, F., Shityakov, S., et al., 2014. Selective suppression of excessive GluN2C expression rescues early epilepsy in a tuberous sclerosis murine model. Nat. Commun. 5, 4563.
Lozovaya, N.A., Grebenyuk, S.E., Tsintsadze, T.Sh, Feng, B., Monaghan, D.T., Krishtal, O. A., 2004. Extrasynaptic NR2B and NR2D subunits of NMDA receptors shape 'superslow' afterburst EPSC in rat hippocampus. J. Physiol. 558, 451–463.
Mao, Z., He, S., Mesnard, C., Synowicki, P., Zhang, Y., Chung, L., Wiesman, A.I., Wilson, T.W., Monaghan, D.T., 2020. NMDA receptors containing GluN2C and GluN2D subunits have opposing roles in modulating neuronal oscillations; potential mechanism for bidirectional feedback. Brain Res. 1727, 146571.
McGuinness, L., Taylor, C., Taylor, R.D.T., Yau, C., Langenhan, T., Hart, M.L., Christian, H., Tynan, P.W., Donnelly, P., Emptage, N.J., 2010. Presynaptic NMDARs in the hippocampus facilitate transmitter release at theta frequency. Neuron 68, 1109–1127.
Meguro, H., Mori, H., Araki, K., Kushiya, E., Kutsuwada, T., Yamazaki, M., Kumanishi, T., Arakawa, M., Sakimura, K., Mishina, M., 1992. Functional characterization of a heteromeric NMDA receptor channel expressed from cloned cDNAs. Nature 357, 70–74.
Monyer, H., Sprengel, R., Schoepfer, R., Herb, A., Higuchi, M., Lomeli, H., Burnashev, N., Sakmann, B., Seeburg, P.H., 1992. Heteromeric NMDA receptors: molecular and functional distinction of subtypes. Science 256, 1217–1221.
Monyer, H., Burnashev, N., Laurie, D.J., Sakmann, B., Seeburg, P.H., 1994. Developmental and regional expression in the rat brain and functional properties of four NMDA receptors. Neuron 12, 529–540.
Morley, R.M., Tse, H.-W., Feng, B., Miller, J.C., Monaghan, D.T., Jane, D.E., 2005. Synthesis and pharmacology of N1-substituted piperazine-2,3-dicarboxylic acid derivatives acting as NMDA receptor antagonists. J. Med. Chem. 48, 2627–2637.
Morris, R.G., Anderson, E., Lynch, G.S., Baudry, M., 1986. Selective impairment of learning and blockade of long-term potentiation by an N-methyl-D-aspartate receptor antagonist, AP5. Nature 319, 774–776.
Mullasseril, P., Hansen, K.B., Vance, K.M., Ogden, K.K., Yuan, H., Kurtkaya, N.L., Santangelo, R., Orr, A.G., Le, P., Vellano, K.M., et al., 2010. A subunit-selective potentiator of NR2C- and NR2D-containing NMDA receptors. Nat. Commun. 1, 1–8.
Park, J., Chávez, A.E., Mineur, Y.S., Morimoto-Tomita, M., Lutzu, S., Kim, K.S., Picciotto, M.R., Castillo, P.E., Tomita, S., 2016. CaMKII phosphorylation of TARPγ-8 is a mediator of LTP and learning and memory. Neuron 92, 75–83.
Park, P., Georgiou, J., Sanderson, T.M., Ko, K.-H., Kang, H., Kim, J., Bradley, C.A., Bortolotto, Z.A., Zhuo, M., Kaang, B.-K., et al., 2021. PKA drives an increase in AMPA receptor unitary conductance during LTP in the hippocampus. Nat. Commun. 12, 413.
Perszyk, R.E., DiRaddo, J.O., Strong, K.L., Low, C.-M., Ogden, K.K., Khatri, A., Vargish, G.A., Pelkey, K.A., Tricoire, L., Liotta, D.C., et al., 2016. GluN2D-containing N-methyl-D-aspartate receptors mediate synaptic transmission in hippocampal interneurons and regulate interneuron activity. Mol. Pharmacol. 90, 689–702.
Pradier, B., Lanning, K., Taljan, K.T., Feuille, C.J., Nagy, M.A., Kauer, J.A., 2018. Persistent but labile synaptic plasticity at excitatory synapses. J. Neurosci. 38, 5750–5758.
Ravikrishnan, A., Gandhi, P.J., Shelkar, G.P., Liu, J., Pavuluri, R., Dravid, S.M., 2018. Region-specific expression of NMDA receptor GluN2C subunit in parvalbumin-positive neurons and astrocytes: analysis of GluN2C expression using a novel reporter model. Neuroscience 380, 49–62.
Rempe, D.A., Bertram, E.H., Williamson, J.M., Lothman, E.W., 1997. Interneurons in area CA1 stratum radiatum and stratum oriens remain functionally connected to

excitatory synaptic input in chronically epileptic animals. J. Neurophysiol. 78, 1504–1515.
Sakimura, K., Kutsuwada, T., Ito, I., Manabe, T., Takayama, C., Kushiya, E., Yagi, T., Aizawa, S., Inoue, Y., Sugiyama, H., 1995. Reduced hippocampal LTP and spatial learning in mice lacking NMDA receptor epsilon 1 subunit. Nature 373, 151–155.
Sanderson, T.M., Bradley, C.A., Georgiou, J., Hong, Y.H., Ng, A.N., Lee, Y., Kim, H.-D., Kim, D., Amici, M., Son, G.H., et al., 2018. The probability of neurotransmitter release governs AMPA receptor trafficking via activity-dependent regulation of mGluR1 surface expression. Cell Rep. 25, 3631–3646 e3.
Sapkota, K., Mao, Z., Synowicki, P., Lieber, D., Liu, M., Ikezu, T., Gautam, V., Monaghan, D.T., 2016. GluN2D N-methyl-D-aspartate receptor subunit contribution to the stimulation of brain activity and gamma oscillations by ketamine: implications for schizophrenia. J. Pharmacol. Exp. Therapeut. 356, 702–711.
Schulz, P.E., Fitzgibbons, J.C., 1997. Differing mechanisms of expression for short- and long-term potentiation. J. Neurophysiol. 78, 321–334.
Shih, P.-Y., Savtchenko, L.P., Kamasawa, N., Dembitskaya, Y., McHugh, T.J., Rusakov, D. A., Shigemoto, R., Semyanov, A., 2013. Retrograde synaptic signaling mediated by K + efflux through postsynaptic NMDA receptors. Cell Rep. 5, 941–951.
Swanger, S.A., Vance, K.M., Acker, T.M., Zimmerman, S.S., DiRaddo, J.O., Myers, S.J., Bundgaard, C., Mosley, C.A., Summer, S.L., Menaldino, D.S., et al., 2018. A novel negative allosteric modulator selective for GluN2C/2D-containing NMDA receptors inhibits synaptic transmission in hippocampal interneurons. ACS Chem. Neurosci. 9, 306–319.
Temi, S., Rudyk, C., Armstrong, J., Landrigan, J.A., Dedek, C., Salmaso, N., Hildebrand, M.E., 2021. Differential expression of GluN2 NMDA receptor subunits in the dorsal horn of male and female rats. Channels 15, 179–192.
Vicini, S., Wang, J.F., Li, J.H., Zhu, W.J., Wang, Y.H., Luo, J.H., Wolfe, B.B., Grayson, D. R., 1998. Functional and pharmacological differences between recombinant N-methyl-D-aspartate receptors. J. Neurophysiol. 79, 555–566.
Volianskis, A., Jensen, M.S., 2003. Transient and sustained types of long-term potentiation in the CA1 area of the rat hippocampus. J. Physiol. 550, 459–492.
Volianskis, A., Bannister, N., Collett, V.J., Irvine, M.W., Monaghan, D.T., Fitzjohn, S.M., Jensen, M.S., Jane, D.E., Collingridge, G.L., 2013a. Different NMDA receptor subtypes mediate induction of long-term potentiation and two forms of short-term potentiation at CA1 synapses in rat hippocampus in vitro: NMDAR subtypes in STP and LTP. J. Physiol. 591, 955–972.
Volianskis, A., Collingridge, G.L., Jensen, M.S., 2013b. The roles of STP and LTP in synaptic encoding. PeerJ 1, e3.
Wang, J.-H., Kelly, P.T., 1997. Attenuation of paired-pulse facilitation associated with synaptic potentiation mediated by postsynaptic mechanisms. J. Neurophysiol. 78, 2707–2716.
Wang, J.X., Irvine, M.W., Burnell, E.S., Sapkota, K., Thatcher, R.J., Li, M., Simorowski, N., Volianskis, A., Collingridge, G.L., Monaghan, D.T., et al., 2020. Structural basis of subtype-selective competitive antagonism for GluN2C/2D-containing NMDA receptors. Nat. Commun. 11, 1–14.
Wigström, H., Gustafsson, B., 1985. Facilitation of hippocampal long-lasting potentiation by GABA antagonists. Acta Physiol. Scand. 125, 159–172.
Yi, F., Bhattacharya, S., Thompson, C.M., Traynelis, S.F., Hansen, K.B., 2019. Functional and pharmacological properties of triheteromeric GluN1/2B/2D NMDA receptors. J. Physiol. 597, 5495–5514.